J Forensic Sci, July 2004, Vol. 49, No. 4
Paper ID JFS2003299
Available online at: www.astm.org

TECHNICAL NOTE

Kathrin Yen,[1] *M.D.; Peter Vock,*[2] *M.D.; Barbara Tiefenthaler,*[1,3] *D.I.; Gerhard Ranner,*[4] *M.D.; Eva Scheurer,*[1] *M.D.; Michael J. Thali,*[1] *M.D.; Karin Zwygart*[5]*; Martin Sonnenschein,*[2] *M.D.; Marco Wiltgen,*[3] *M.D.; and Richard Dirnhofer,*[1] *M.D.*

Virtopsy: Forensic Traumatology of the Subcutaneous Fatty Tissue; Multislice Computed Tomography (MSCT) and Magnetic Resonance Imaging (MRI) as Diagnostic Tools*

ABSTRACT: Traumatic lesions of the subcutaneous fatty tissue provide important clues for forensic reconstruction. The interpretation of these patterns requires a precise description and recording of the position and extent of each lesion. During conventional autopsy, this evaluation is performed by dissecting the skin and subcutaneous tissues in successive layers.

In this way, depending on the force and type of impact (right angle or tangent), several morphologically distinct stages of fatty tissue damage can be differentiated: perilobular hemorrhage (I), contusion (II), or disintegration (III) of the fat lobuli, and disintegration with development of a subcutaneous cavity (IV).

In examples of virtopsy cases showing blunt trauma to the skin and fatty tissue, we analyzed whether these lesions can also be recorded and classified using multislice computed tomography (MSCT) and magnetic resonance imaging (MRI). MSCT has proven to be a valuable screening method to detect the lesions, but MRI is necessary in order to properly differentiate and classify the grade of damage. These noninvasive radiological diagnostic tools can be further developed to play an important role in forensic examinations, in particular when it comes to evaluating living trauma victims.

KEYWORDS: forensic science, soft tissue trauma, reconstruction, forensic radiology, forensic pathology, virtopsy, CT, MR, pathologic-radiologic correlation, fat tissue

Traumatic lesions of the subcutaneous fatty tissue provide important clues for forensic reconstruction (1,2). During conventional autopsy, incision and dissection of the skin and subcutaneous tissues in successive layers permit their evaluation; spectrophotometry and diaphanoscopy can also be used (3,4). By clinical inspection and nondestructive analysis, however, it is less easy to detect traumatic alterations of the fatty tissue.

White fatty tissue is a particular form of connective tissue. It is a layer of varying thickness that consists of overlapping fat lobuli. Each lobulus contains monovacuolar fatty cells, each containing one large drop of fat, separated from each other by fibrous tissue. The cells are nourished by capillaries arrayed "like the branches of a grape leading to its berries" (5). Due to their hydrophilic cell membrane and oily content, they are very resistant to pressure, which is the reason they are present as isolation and padding all over the body.

Until now, only Walcher and Patscheider have attempted to differentiate and grade the lesions occurring in fatty tissue. Walcher described subcutaneous cavities and also differentiated between localized disruption and tearing and large-scale tissue disintegration and décollement-like cavities occasioned by tangential force as seen in road accidents (1). Patscheider further developed the idea of different grades of fatty tissue trauma and described cases of hemorrhage observed after motor vehicle accidents which were distinct from both disintegration and décollement-like lesions (2). Until today, a well-defined classification of fatty tissue trauma grades is still nonexistent.

In the course of our previous studies (6) we demonstrated that magnetic resonance imaging is sensitive enough to detect soft tissue lesions. In the following, we wish to determine whether four various stages of fatty tissue damage, which are to be defined in the present work, can be diagnosed and differentiated using MSCT/MRI.

Material and Methods

Four selected cases from the "Virtopsy" study with findings not analyzed in our earlier publication (6) are presented.

Case 1 (excerpt from the protocol)—A 64-year-old woman was hit by a car while crossing a street. Central respiratory paralysis

[1] Institute of Forensic Medicine, University of Bern, Switzerland.
[2] Institute of Diagnostic Radiology, University of Bern, Switzerland.
[3] Institute of Medical Informatics, Statistics and Documentation, University of Graz, Austria.
[4] CT/MR-Center, Graz-Geidorf, Austria.
[5] Department of Clinical Research, Magnetic Resonance Spectroscopy and Methodology, University of Bern, Switzerland.

* Supported by grants from the Gebert-Ruef-Foundation, Switzerland and from the Government of Vorarlberg, Austria.

Received 6 Sept. 2003; and in revised form 21 Jan. 2004; accepted 4 Feb. 2004; published 26 May 2004.

following fracture of the second cervical vertebra and pulmonary fat embolism led to death four days after the event.

External examination revealed a band-shaped, 12-cm subcutaneous hemorrhage across the outside of the left thigh. Forty-five cm above the sole, another pronounced subcutaneous hemorrhage across the lateral lower left leg was found, close to the back of the knee, surrounded by a palm-sized, diffuse bluish hemorrhage.

Case 2 (excerpt from the protocol)—A 20-year-old man collided with a car while riding his bicycle. Immediate death occurred at the accident site by central paralysis following brainstem rupture.

On the right dorsal and medial thigh, one hand's width below the gluteal fold, there was a palm-sized bluish translucent hemorrhage. Another 4 × 4 cm bluish subcutaneous hemorrhage presented on the inner side of the right knee.

Case 3 (excerpt from the protocol)—A 94-year-old man was hit by a car. He died six days after the accident from central paralysis following extensive cerebral trauma.

On the inner side of the left knee, there was a pronounced 10 × 10 cm subcutaneous hemorrhage with blotchy, brownish hematomas spreading down the lower leg. The right hip appeared macroscopically intact.

Case 4 (excerpt from the protocol)—A 45-year-old woman died four and a half hours after falling into a glacier cleft. Cause of death was hypothermia and positional asphyxiation. The external examination revealed a rounded bluish hemorrhage with a diameter of approximately 12 cm along the exterior of the right upper arm.

All the deceased first underwent an external examination. After this, postmortem MSCT examinations of all three body cavities and selected areas of the extremities (GE Lightspeed QX/i unit; General Electric Medical Systems, Milwaukee, WI) were performed with the data being recorded axially at 4 × 1.25 mm collimation for a slice thickness of 1.5 mm. In case 2, the lower extremities were excepted from the MSCT examination. Following this, MRI of the head, thorax and abdomen was performed; scanning included several individually involved areas of the extremities, using surface coils in cases 1 and 2 (GE 1.5 T Signa Echospeed Horizon, version 5.8 unit; General Electric Medical Systems, Milwaukee, WI). The protocol included standard T2-weighted sequences (FSE, TR/TE 4000/90 ms) with fat saturation, and T1-weighted sequences (SE, TR/TE 400/15-20 ms). The slice thickness was 5 mm with gaps of 1 mm as overview. The selective images with surface coil on the fatty tissue were taken with a slice thickness of 2–3 mm with gaps of 0.2–0.3 mm. Additional sequences were used individually as needed, e.g., using the same parameters in an additional plane, STIR, or gradient echo sequences.

The complete radiological data—evaluated by board-certified radiologists—were available before the conventional autopsy in cases 1 through 4. During each autopsy, a layered soft-tissue dissection was performed and samples of fatty tissue taken from selected areas of the extremities were examined microscopically.

The Virtopsy project is at present in an early research phase. Therefore it is impossible to give exact information on the expected cost, time required and practicality of this method when it becomes implemented in routine forensic practise; we can only report on our actual research details. In Bern, the radiological examinations are performed in close collaboration with the local university hospital, and our experiences with this organizational structure are excellent. Nevertheless, it is imaginable that forensic institutions might generate other possibilities (e.g., keeping own scanners, which is already done by some forensic institutes who own a CT scanner, or sharing the machines). Reflecting the rapid development of radiological imaging techniques in the previous years and the decreasing trend of prices for CT and MR examinations, a development of postmortem imaging similar to the implementation of DNA technology into the field of forensic sciences is possible.

Cost—The actual costs for examination of one case with the Virtopsy method (transportation of the body, whole body MSCT and MRI of the head, thorax and abdomen plus selected regions of special interest) add up to about twice as much as a "classical" autopsy. If special techniques are applied (e.g., the use of surface coils, special time-consuming MR protocols), scanning costs mount up to one more third. Within the Virtopsy network, a radiologist is part-time employed.

Time—The time required for pre-radiology preparation of the deceased (i.e., wrapping the body into special artifact-free body bags) is in the range of ten minutes. Transportation to the university hospital, which is performed by a local mortician, takes a few minutes as does the transportation between MSCT and MRI units. The whole-body MSCT examination (including the correct positioning of the body on the console) lasts about 15 to a maximum of 30 minutes. MRI is far more time-consuming, depending on the regions of interest which will be scanned and on the number of applied MR protocols per region. Within the Virtopsy project, almost all bodies undergo head, thorax and abdominal MRI (using the head and body coils and various protocols) which together require up to two hours, again including the positioning of the body in the MR scanner. Depending on accessory regions of interest or special protocols, time exposure might extend to four or a maximum of five hours.

Practicality—Within the last two years, the Virtopsy method has turned out to be very practicable in the actual organizational structure of the Forensic and Radiological units. Limiting factors are the need to do the MSCT and MRI scanning in the evenings so as not to disturb routine clinical casework; therefore, a Virtopsy assistant as well as a medical-technical assistant have to be on duty in the evening hours. The required time of three to four hours per Virtopsy examination and the time restrictions resulting from the use of hospital scanners limit the feasible number of deceased to be examined by postmortem imaging. Radiologic evaluation of the imaging data is actually performed while scanning and again after autopsy.

Results

In the following, the macro- and microscopic autopsy results obtained after layered soft tissue dissection are listed and compared with the results from MSCT and MRI.

Case 1

Autopsy—Macroscopically, an incision along the exterior left thigh showed contusion of fat lobuli with surrounding red-brownish discoloration. A disintegration zone of mush-like consistency lay beside this. More distally, a subcutaneous décollement-like cavity filled with blood and liquefied fat was found, with several strands of connective tissue bridging the defect along its edges. The lesion of the left knee was a contusion of the fatty tissue with the formation of a small cavity. The surrounding tissue was intact but showed perilobular hemorrhage.

Histology—Microscopically, the perilobular hemorrhage was visible as blood surrounding intact fat lobuli within which the tissue structures remained undamaged. Contusion was characterized by bleeding around and within the lobular structure enclosing intact fat cells, while the lobular structure itself remains undamaged. In fatty tissue disintegration, however, the connective tissue structuring the

lobuli was disrupted; fatty cells were dislocated and partially destroyed. Inside the subcutaneous defect cavities, islands of fat cells and drops of liquid fat were visible in the pool of blood.

MSCT—The disintegration zone on the outside of the left thigh appeared as an irregular, poorly defined structure. The subcutaneous defect cavity was easily recognizable by its liquid content and presented as a well-defined, hyperdense (compared to the surrounding fat tissue), homogenous formation adhering to the fascia of the m. vastus lateralis. The contusions on the left thigh and the perilobular hemorrhages alongside the left knee were practically invisible.

MRI—The hemorrhages around the left knee appeared as hypo- (T1) or hyperintense (T2) signal alterations with a crosshatch streaky pattern corresponding to the connective tissue filaments within the perilobular hemorrhage zone. The fatty tissue contusions on the knee and lateral thigh read as nodular, clouded signal alterations that—unlike the perilobular hemorrhage—lacked a clear demarcation to the surrounding tissue. Disintegration and contusion could not be differentiated from each other in the transition boundary; however, in the central, more pronounced disintegration areas, the nodular cloudy signals showed a confluent pattern that allowed a reliable diagnosis. Subcutaneous cavities, on the other hand, appeared very clearly as homogenous, well-defined accumulations of pooled liquid and were easily classified.

Case 2

Autopsy—Macroscopically, the posterior and medial area of the right thigh showed contusion of the fat lobuli with surrounding red-brownish discoloration and around this a hemorrhage surrounding intact yellow fat lobuli. On the left leg, colocating with the previously described posterior subcutaneous discoloration, a large hemorrhage zone was observed. The left knee revealed a disintegration area with formation of a subcutaneous defect cavity filled with blood and liquefied fat and bridged by many tissue filaments along its edges.

Histology—The microscopic appearance of the various lesions was identical to those described in detail in Case 1.

MRI—The contusion zone along the right thigh was particularly visible in the inverted T1-image and appeared as a cloudy, poorly demarcated signal alteration with opacification of the fat lobuli. The surrounding interlobular hemorrhage showed a crosshatched streaky pattern similar to that found on MRI in case 1.

The hemorrhages along the left knee, in contrast, appeared as well-defined, linear-patterned signal alterations. The defect cavity was easily recognizable by its liquid accumulation within the tissue; the pronounced contrast pattern distinguished it from the surrounding area of disintegration with its diffuse pattern of increased fat signal.

Case 3

Autopsy—Here, too, contusions of the right hip and left knee macroscopically appeared as red-brownish discolorations of the fatty tissue. A disintegration zone of the left knee showed destroyed fat lobuli and the tissue had a gelatinous, mush-like consistency.

Histology—The results of the microscopic examination corresponded to those in case 1.

MSCT—The contusion of the right hip was not visible in the MSCT examination. The left knee showed a barely perceptible structure alteration in the disintegration area.

MRI—The fatty tissue layers were thinner in the contusion region at the right hip than in the surrounding areas; also, they appeared as cloudy and poorly demarcated signal alterations. The left knee showed nodular cloudy signals which were poorly demarcated and partially confluent; the differentiation between contusion or disintegration of the fat lobuli in this region was not sufficient by means of MR imaging.

Case 4

Autopsy—Macro- and microscopically, there was only an isolated red-brownish contusion of fatty tissue situated in the upper right arm.

Histology—Contusion as described in Case 1.

MSCT—The injured area was not identifiable in the MSCT examination; however, the quality of the examination was poor due to stripe artifacts.

MRI—The contusion appeared as a cloudy and poorly demarcated signal reduction in T2 and signal increase in T1. The fat lobuli had a milky and diffuse appearance.

Discussion

The pathology of fatty tissue trauma usually receives little attention in clinical medicine (7,8). Historically, this is not surprising, since even Hyrtl (5) described fatty tissue as "that human tissue most despised by all anatomists, for the reason that, because of it, their work—preparing specimens—is hindered, disturbed or rendered altogether impossible . . . ."

This is why there have been no structured concepts and discussions about the morphology and classification of traumatic lesions of the subcutaneous fatty tissue. Even in the forensic sciences, such writing is rare (1,2). Bohnert (4) and Horisberger (3) have addressed this subject in the more recent past, yet, despite their work, criteria for the classification of the degrees of traumatic damage to fatty tissue are lacking to date.

Based on the work of Walcher and Patscheider, we define four degrees of fatty tissue damage according to macro- and microscopical criteria (Fig. 1 and Table 1). This grading is forensically important when it comes to determining the exact location and the extent of a traumatic blunt force impact to the body.

Grade I: Perilobular Hemorrhage (Fig. 2*a*, *b*; Cases 1 and 2)

After a slight trauma, reddish-blue hemorrhages appear around the individual fat lobuli, primarily located within the connective tissue septum, while the lobuli themselves remain intact and retain their yellow color. Perilobular hemorrhage occurs not only from direct traumatization of the fatty tissue, but also as a consequence of passive bleeding into the fat tissue structures from a close-by impact location.

Grade II: Contusion of the Fat Lobuli (Fig. 3*a*, *b*; Cases 1–4)

As the violence of the trauma increases, the subcutaneous tissue takes on a blotchy reddish-brown discolored appearance due to—microscopically visible—hemorrhages between and within the fat lobuli (perilobular and pericellular hemorrhage); here, too, the structure of the lobuli remains intact. Macroscopically, this type of discoloration is characteristic for the area of direct impact. In contrast to perilobular hemorrhage, a contusion of the fatty tissue always indicates a direct traumatic impact and is therefore of fundamental importance regarding the forensic reconstruction of the event.

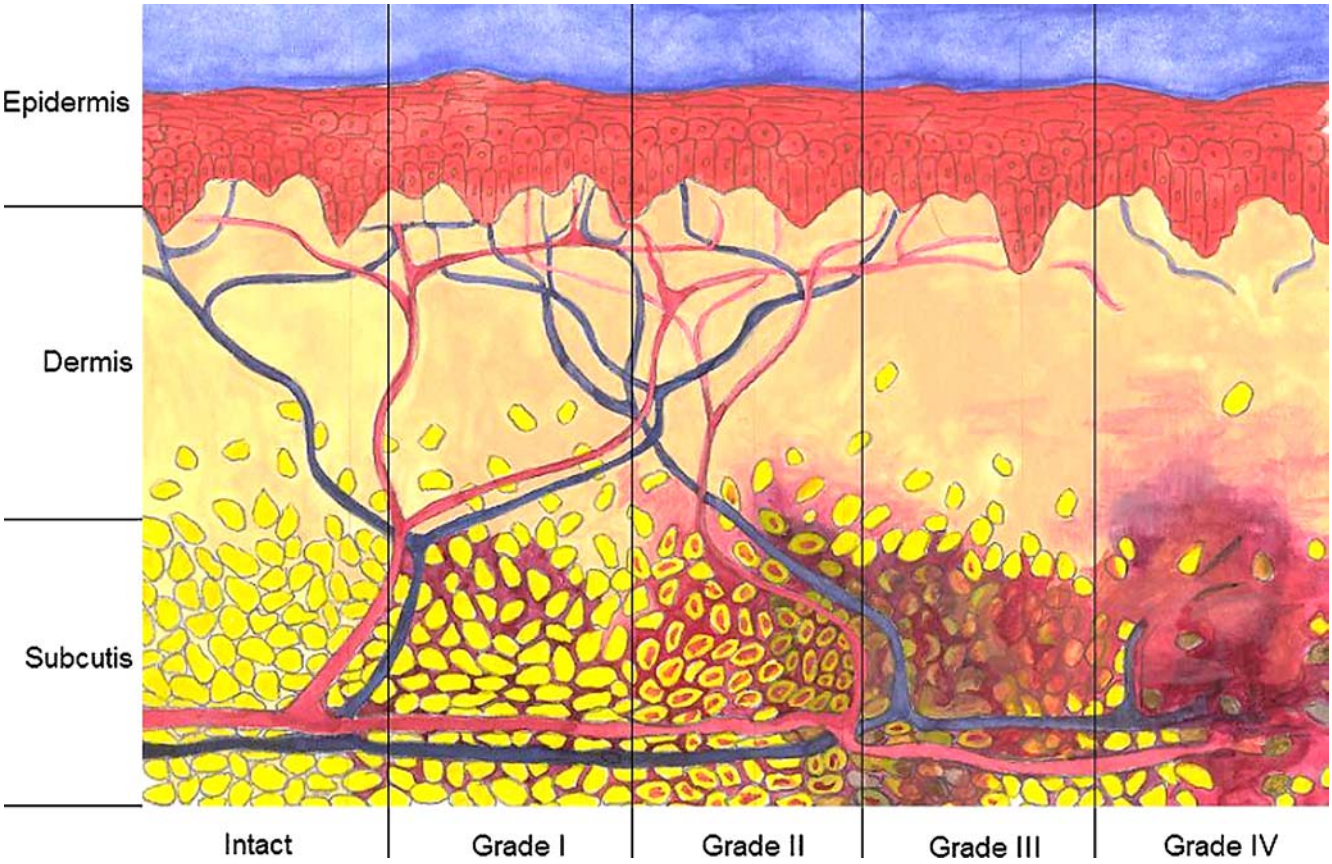

FIG. 1—*Schematic illustration of the four fatty tissue trauma grades. Grade I: Perilobular bleeding. Hemorrhage is found around the yellow, intact fat lobuli. Grade II: Contusion of the fat lobuli. Bleeding around and inside the mainly intact lobuli leads to a characteristic red-brownish discoloration at the contusion site. Grade III: Disruption of fatty tissue structures. A release of liquid fat resulting from the damage of the lobular architecture and hemorrhage at the location of the injury gives the disruption a mush-like, red-brown appearance. Grade IV: Crush cavity. A cavity formation filled with blood and liquid fat is present in the subcutaneous tissue; the fat lobuli are mainly destroyed.*

Grade III: Disintegration of Fat Lobuli (Fig. 4*a*, *b*; Cases 1–3)

The next stage corresponds to a local disintegration of the fat lobuli. The septae between the lobuli and the fat cell membranes are partially destroyed, hemorrhage appears inside the lobuli and around the individual fat cells, and liquefied fat which is visible as "grease drops" is released. Macroscopically, the subcutaneous fat in this area has a gelatinous, mush-like consistency.

Grade IV: Crush Cavity (Fig. 5*a*, *b*; Cases 1 and 2)

Following violent trauma, the destruction of fatty tissue is so pronounced that a subcutaneous cavity is formed in which blood and liquefied fat collect. Microscopically, this is visible as a pool of blood containing drops of fat and released islands of fatty cells. If the force acts tangentially, the disruption can be important enough to cause a décollement-like lesion when the entire layer of subcutaneous fat disconnects from the fascia. In this case, Metter (9,10) uses the term "impact décollement." The term décollement itself, however, should be reserved for the dislocation of the subcutaneous fatty layer through tangential shear (as seen in some road accidents), since in this case the layer of fatty tissue itself remains relatively unharmed and hardly ever forms bridges of connective tissue within the cavity.

A clear-cut demarcation of fatty tissue injury into the preceding four grades is not always possible as the findings may overlap between the individual gradings.

To date, the few clinical publications dealing with the application of MRI/MSCT techniques to the diagnosis of trauma of the subcutaneous fatty tissue are of little relevance for forensic practice (7,8). Isolated cases of postmortem MRI/MSCT analysis of soft tissue have been reported (6,11,12).

Our experiences with digital radiological imaging have now demonstrated that MSCT is not sufficient to classify the degrees of fatty tissue trauma (Table 1). It is essentially based on the density difference between fat (around −80 to −200 Hounsfield Units, HU) and the large group of fresh blood and nearly all soft tissues (around 20 to 65 HU). Obviously, with intact fat lobuli the density of the subcutaneous fat is not significantly increased, and grades I and II lesions accordingly were not visible. In grade III lesions the MSCT patterns appeared as cloudy, ill-defined signal alterations (Fig. 4*c*). Only grade IV damage (Fig. 5*c*) with its accumulation of liquid in the tissue was easily diagnosed and differentiated from normal fat and lower grade lesions. Nevertheless, we can conclude that MSCT, due to its speed, is useful as a screening tool for the detection of subcutaneous fatty tissue trauma.

The MRI results are more promising, since all four types of lesions could be diagnosed and to a reasonable extent differentiated from each other (Table 1). Perilobular hemorrhage (grade I, Fig. 2*c*) and contusions (grade II, Fig. 3*c*) were distinguishable since the hemorrhage showed a crosshatched, streaky, well-defined hyper- (T2) or hypointense (T1) pattern while contusions showed as cloudy, nodular, ill-defined signal alterations.

TABLE 1—*Results.*

	Macroscopic Results	Microscopic Results	MRI	MSCT
Grade I Perilobular hemorrhage	Perilobular hemorrhage surrounding intact, yellow fat lobuli. Fig. 2*a*	Hemorrhage into the connective tissue surrounding intact fat lobuli. Scarcely any bleeding within the lobuli, fat cells remain intact. Fig. 2*b*	Depending on the sequence, perilobular hemorrhage shows as hypo- (T1) or hyperntense (T2) crosshatched streaky well-defined signal alteration. Fig. 2*c*	Not recognizable.
Grade II Contusion of the fat lobuli	Blotchy reddish-brown discoloration of fat lobuli at the impact site. Fig. 3*a*	Perilobular hemorrhage as well as hemorrhage inside the structurally intact fat lobuli surrounding undamaged fat cells. Fig. 3*b*	Nodular, cloudy hypo- (T1) or hyperintense (T2) signal alteration in the subcutaneous fatty tissue with poor demarcation. The contusion areas are easily distinguishable from the surrounding hemorrhage. Fig. 3*c*	Not recognizable.
Grade III Disintegration	Destruction of the fat lobuli with disintegration of the lobular architecture and release of liquefied fat. The subcutaneous fat at the impact site has a gelatinous, mush-like appearance. Fig. 4*a*	The connective tissue filaments surrounding the fat lobuli are largely destroyed. Hemorrhage between and within the lobuli. Fig. 4*b*	As in II; confluence in the center of the nodular-cloudy structures, demarcation stays ill-defined. Differentiation between disintegration zones and isolated contusion is not always possible in the MRI, particularly when the disintegration is limited. Fig. 4*c*	Irregularly distributed signal increases in the subcutaneous fat. Fig. 4*d*
Grade IV Crush cavity	Cavity formation within the subcutaneous tissue following disintegration of fat lobuli with resulting connective tissue bridges; the cavity is filled with pooled blood and liquefied fat (visible as "grease drops" in the blood). Frequent surface hemorrhage along the base of fat lobuli in the plane of detachment from the fascia. Fig. 5*a*	As seen in III, accompanied by the formation of a blood-filled cavity. The pool of blood contains groups of fat cells released from the fat lobules and coalesced fat. Fig. 5*b*	Well-demarcated, irregular-shaped liquid collection within the subcutaneous fat, hypo- or hyperintense liquid signal depending on the MR sequence. Fig. 5*c*	As seen in III; larger liquid accumulations in the fatty tissue show a clear boundary and are easily recognized in MSCT. Fig. 5*d*

MRI also allowed discrimination between disintegration of fat lobuli (grade III, Fig. 4*d*) and the formation of defect cavities (grade IV, Fig. 5*d*), the latter appearing as a well-defined, homogenous liquid formation within the surrounding tissue while the former was characterized by confluent, nodular, and cloudy signal alterations.

With regard to the MR protocols used in this study, we can conclude that T1 sequences are particularly well suited for postmortem (25°C body core temperature) imaging of subcutaneous fatty tissue lesions grades I and II; due to the larger amounts of released liquids, grades III and IV are presenting well in T2 sequences with fat saturation. The use of additional surface coils, as done in cases 1 and 2, enables even better image resolution.

Using MRI, the main difficulties lay in differentiating between grade II and grade III lesions. As shown in case 1, distinguishing a contusion from a disintegration was challenging, since both lesions were easily visible but to some extent shared a cloudy, nodular signal pattern, particularly in the transition zones. Minor disintegrations could hardly be discerned from serious contusions; only the more important disintegrations were easily classified since they had a clear central confluence not visible in the more disparate pattern of contusions.

The reasons for these diagnostic difficulties lie not only with the continuum of tissue lesions including intermediate stages, but also with the resolution capacity of current clinical MR scanners. With the advent of High-Tesla scanners and high-field MRI in routine radiological practice, we can expect much better resolution and diagnostic potential in the near future (13).

Notwithstanding the potential of MRI in the forensic pathology of fatty tissue trauma, there remain many challenges for the future. Among these, the exact geometric lesion mapping in the course of forensic reconstruction in order to determine the precise location of the point of impact, or the correlation of particular lesions to motor vehicle structures, are just two of them. Considering the potential of 3-D reconstruction of trauma patterns for court proceedings in the near future, the exact mapping of skin, tissue, and bone lesions will be of particular importance. In our cases, the use of surface coils, despite their improved local geometrical resolution, was an impediment to the precise mapping of "damage geometry" since only one region on one half of the body could be analyzed at one

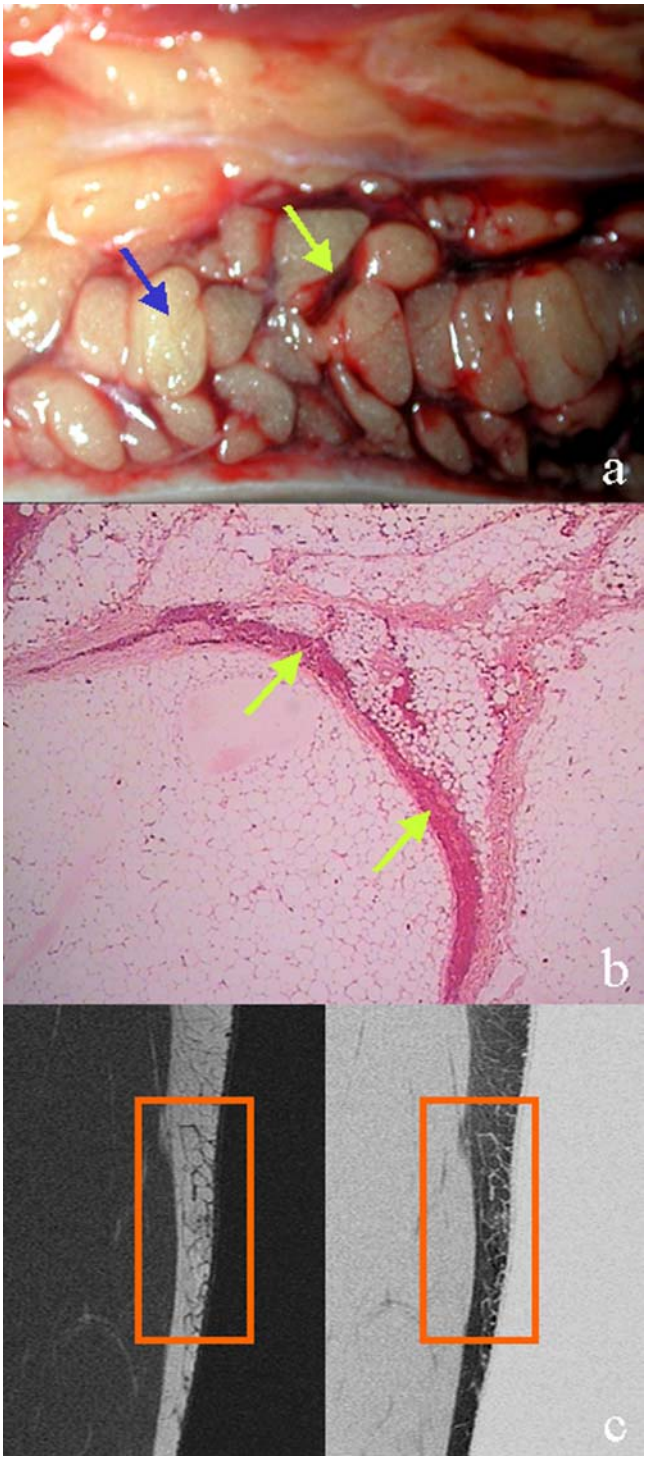

FIG. 2—*Grade I of fatty tissue injury: perilobular bleeding (case 2).* (a) *Findings at autopsy showing hemorrhage* (green arrow) *around the intact, yellow fat lobuli* (blue arrow). (b) *Corresponding histological findings show erythrocytes along the septae between the mainly intact fat lobuli* (arrows). (c) *Coronal T1-weighted MR image of the right thigh indicating hemorrhage as hypointense crosshatched, streaky signal alteration. This finding of a reticular pattern caused by thickened interlobular septae is more easily detectable in the inverted image* (right).

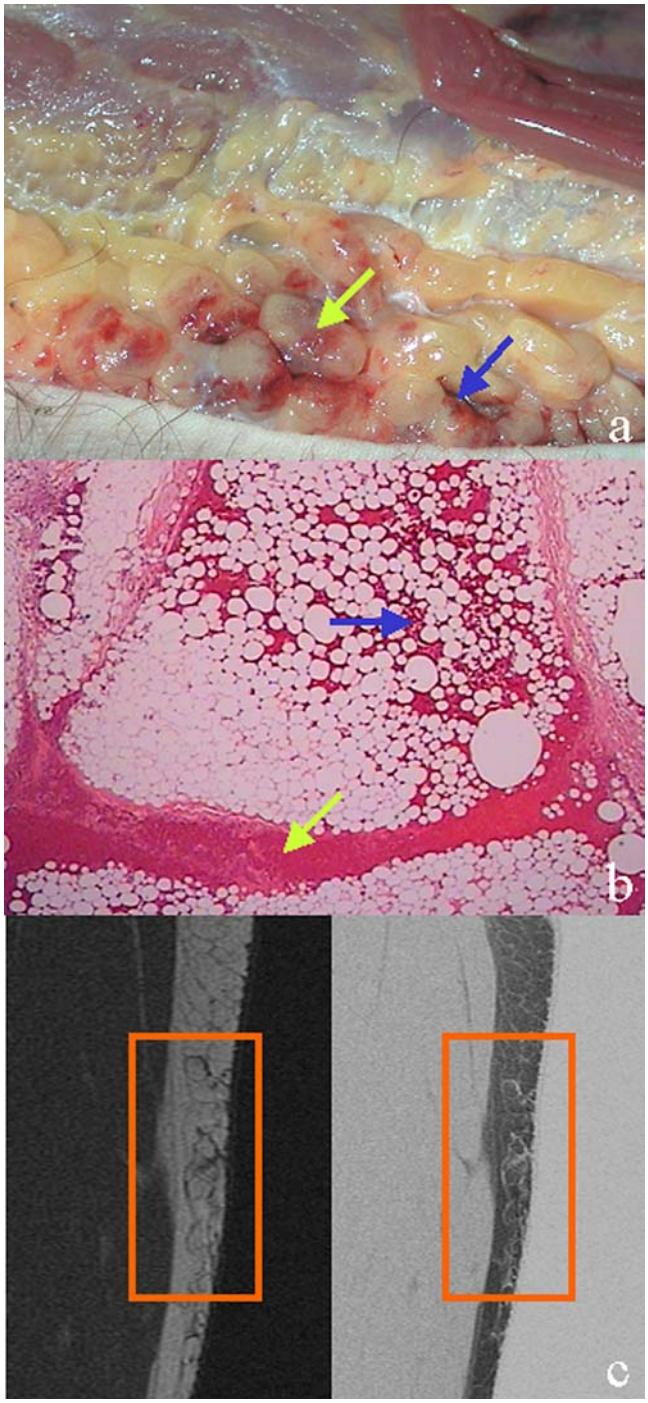

FIG. 3—*Grade II: contusion of the fat lobuli (case 2).* (a) *At autopsy, hemorrhage is located both around* (blue arrow) *and within* (green arrow) *the fat lobuli at the contusion site giving these a characteristic flecked, red-brown appearance.* (b) *Histological correlation to* (a). *Erythrocytes can be seen around the fat lobuli* (green arrow) *as well as between the fat cells within each individual lobule* (blue arrow). (c) *Contusion of the right thigh; in addition to the findings seen in Fig. 2, a nodular, cloudy hypointense signal alteration appears in the T1-weighted MR image* (right: inverted image).

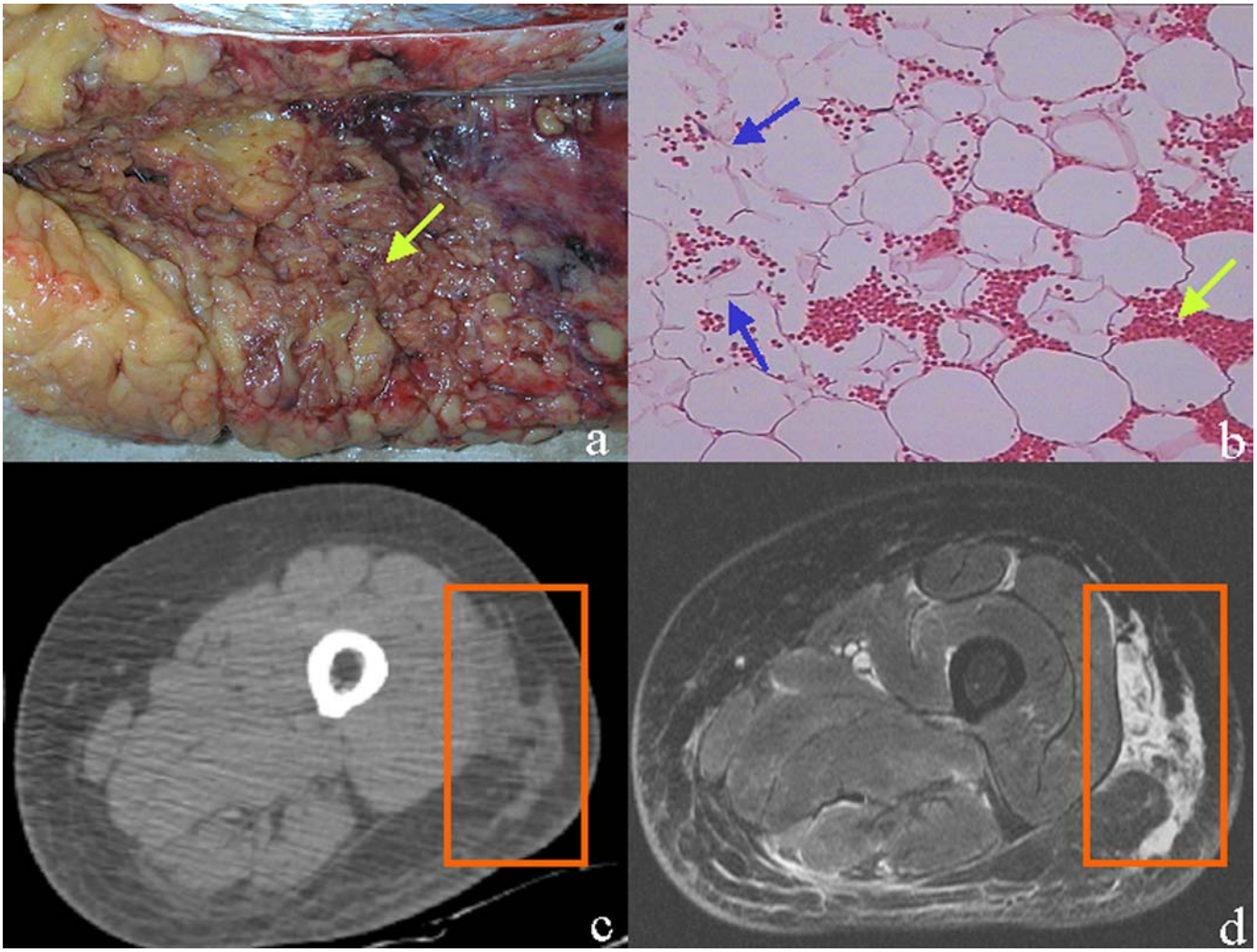

FIG. 4—*Grade III: disruption of fatty tissue (case 1).* (a) *At autopsy, disruption is characterized by a mush-like, red-brown appearance* (arrow) *which results from the damage of lobular fatty tissue architecture and release of liquefied fat.* (b) *Histological examination showing, in addition to the pericellular hemorrhage* (green arrow)*, destruction of some fat cells with disruption of the internal lobular structure* (blue arrow). (c) *MSCT reveals an irregularly distributed density increase in the injured region.* (d) *The T2-weighted, fat saturated axial MR image shows a confluence of the nodular-cloudy signal alterations.*

time. Although we attempted to remedy this by placing artifact-free markers on selected and measured body areas to help orientation, the results were not convincing, especially considering the resolution and image quality necessary for the documentation of forensic cases.

Lastly, we also need to address the influence of subcutaneous emphysema, putrefaction and edema on the imaging of fatty tissue lesions and to examine the signal pattern of livid spots in MSCT and MRI since it is unknown whether they can alter or interfere with the signals from traumatic lesions.

Conclusions

The here presented grading of injury patterns based upon morphological criteria may be taken as an initial step for developing a systematic classification of injuries based upon radiological imaging findings. The comparison of digital radiological imaging techniques shows that MRI is well suited to help recognize and classify the lesions of fatty tissue that are important for forensic reconstruction. MSCT has its place as a rapid screening tool but not as a sensitive diagnostic method. Despite the fact that the traumatology of subcutaneous fat does not play an important role in clinical diagnostic radiological practice, the use of MRI will vastly enrich the diagnostic possibilities in forensic clinical cases where pathological analysis is not available. It remains to be clarified whether the ongoing technical improvement of imaging methods and/or the combination of MR/MSCT with color surface scanning can nondestructively equal conventional autopsy in detecting and classifying subcutaneous tissue injury.

Acknowledgments

We offer particular thanks to the Gebert-Ruef-Foundation and the Vorarlberg Federal Government for their financial support of this project.

We also thank Urs Königsdorfer and Roland Dorn, of the Institute of Forensic Medicine in Bern, for their support with data acquisition during the autopsies and Therese Perinat for having prepared the sample slides. Furthermore, our thanks go to Elke Spielvogel and Suzanne Horlacher, Department of Radiology, University of Bern, for their help with the MSCT examinations, to Robert Yen for the illustration of the traumatologic findings, and to Nathalie Frickey,

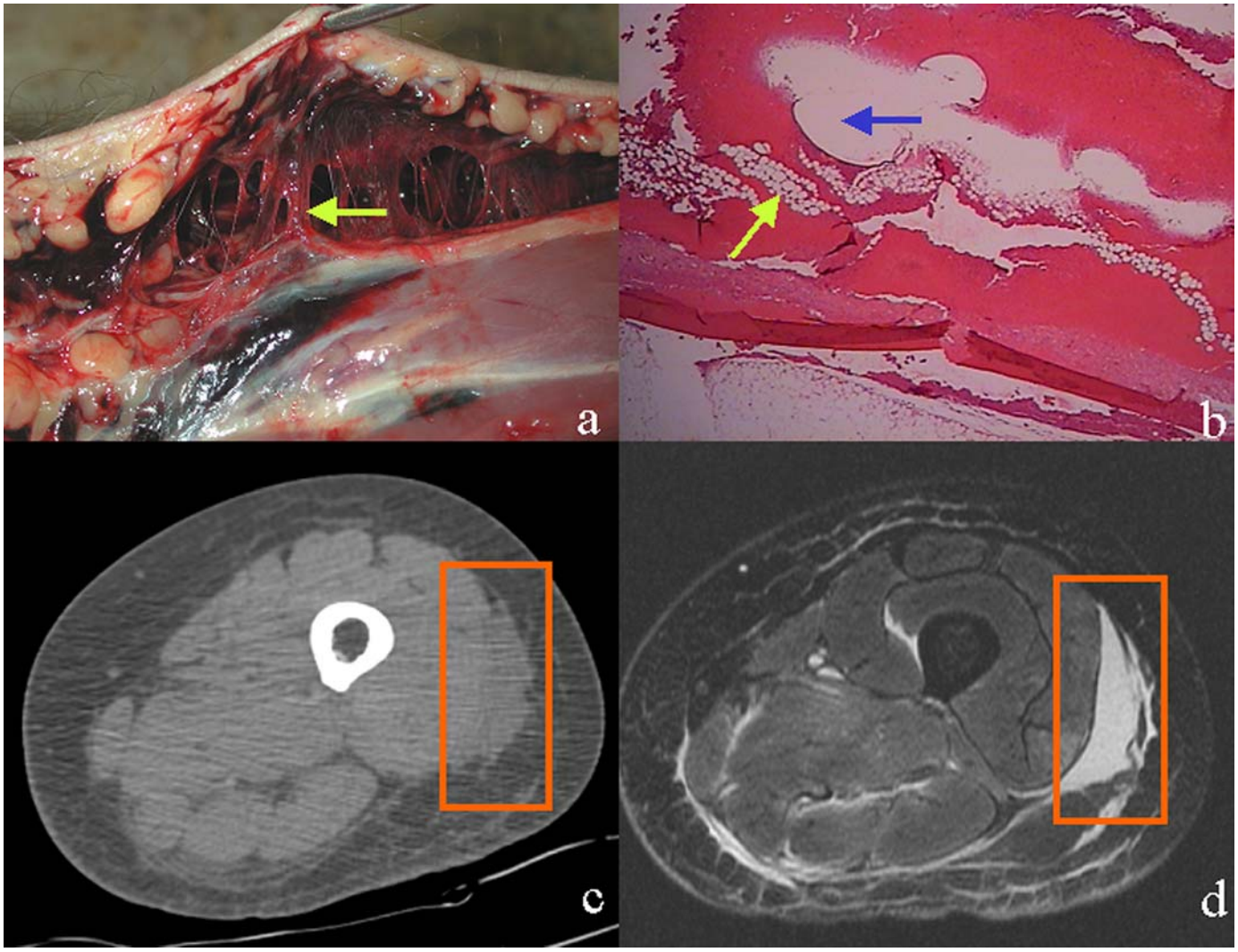

FIG. 5—*Grade IV: crush cavity (case 1).* (a) *A cavity formation in the fatty tissue found at autopsy. Substantial destruction of underlying tissues is present such that lifting of the skin reveals numerous connective tissue bridges* (arrow). (b) *Corresponding histological finding; the cavity is filled with blood within which groups of cells released from the fat lobules* (green arrow) *and coalesced fat* (blue arrow) *are clearly seen.* (c) *MSCT image of the left thigh. A larger blood accumulation can be seen in the fat tissue layers.* (d) *Same location in the axial FSE T2-weighted and fat-saturated MR image. The well-demarcated homogenous pool of blood is clearly recognizable.*

Department of Anesthesiology, AKH Vienna, for the translation of this manuscript.

References

1. Walcher K. Medizinische und naturwissenschaftlich-kriminalistische Untersuchungen bei Verletzungen durch stumpfe Gewalt. In: Abderhalden E, editor. Handbuch der biologischen Arbeitsmethoden. Berlin, Wien: Urban und Schwarzenberg, 1934;637–76.
2. Patscheider H. Ueber Anprallverletzungen der unteren Gliedmassen bei Strassenverkehrsunfällen. Fortschr Med 1967;2(85):47–50.
3. Horisberger B, Krompecher T. Forensic diaphanoscopy: how to investigate invisible subcutaneous hematomas on living subjects. Int J Legal [PubMed] Med 1997;110(2):73–8.
4. Bohnert M, Baumgartner R, Pollak S. Spectrophotometric evaluation of the colour of intra- and subcutaneous bruises. Int J Legal Med [PubMed] 2000;113(6):343–8.
5. Fett HJ. In: Hyrtl J, editor. Lehrbuch der Anatomie des Menschen. Wien: Wilhelm Braumüller, 1889;111–7.
6. Thali MJ, Yen K, Schweitzer W, Vock P, Boesch C, Ozdoba C, et al. Virtopsy, a new imaging horizon in forensic pathology: virtual autopsy by postmortem multislice computed tomography (MSCT) and magnetic resonance imaging (MRI)—a feasibility study. J Forensic Sci 2003 [PubMed] Mar;48(2):386–403.
7. Lacotte B, De Mey A, Coessens B. Trauma of the fatty tissue. Acta Chir Belg 1994;94:17–20. [PubMed]
8. Meggitt BF, Wilson JN. The battered buttock syndrome—fat fractures. A report on a group of traumatic lipomata. Br J Surg 1972;59(3):165–9.
9. Metter D. Decollement as initial collision injury. Z Rechtsmed 1980; 85(3):211–9. [PubMed]
10. Metter D. Fussgaenger-PKW-Unfaelle bei Kollisionsgeschwindigkeiten über 70 km/h. Beitr Gerichtl Med 1984;42:319–27. [PubMed]
11. Farkash U, Scope A, Lynn M, Kugel C, Maor R, Abargel A, et al. Preliminary experience with postmortem computed tomography in military penetrating trauma. J Trauma 2000;48(2):303–8. [PubMed]
12. Donchin Y, Rivkind AI, Bar-Ziv J, Hiss J, Almog J, Drescher M. Utility of postmortem computed tomography in trauma victims. J Trauma 1994;37(4):552–5. [PubMed]
13. Thali MJ, Dirnhofer R, Potter K. Forensic MR microscopy: analysis of blunt force trauma in skin and subcutaneous fat tissue. Proc Int Soc Magn Reson Med 2003;11.

Additional information and reprint requests:
Kathrin Yen, M.D.
Institute of Forensic Medicine , University of Bern
Buehlstrasse 20
CH-3012 Bern, Switzerland
E-mail: yen@irm.unibe.ch